A&A 509, A64 (2010)
DOI: 10.1051/0004-6361/200912863

Astronomy & Astrophysics

Near-infrared colours of active galactic nuclei

S. Kouzuma and H. Yamaoka

Graduate School of Sciences, Kyushu University, Fukuoka 812-8581, Japan
e-mail: kouzuma@phys.kyushu-u.ac.jp

Received 10 July 2009 / Accepted 9 October 2009

ABSTRACT

We propose near-infrared colour selection criteria to extract active galactic nuclei (AGNs) using the near-infrared colour-colour diagram (CCD) and predict near-infrared colour evolution with redshift. We first cross-identify two AGN catalogues with the 2MASS Point Source Catalogue, and confirm both the loci of quasars/AGNs in the near-infrared CCD and redshift-colour relations. In the CCD, the loci of over 70−80% of AGNs can be distinguished from the stellar locus. To examine the colours of quasars, we simulate near-infrared colours using the Hyperz code. Assuming a realistic quasar SED, we derive simulated near-infrared colours of quasars with redshift (up to $z \sim 11$). The simulated colours can reproduce not only the redshift-colour relations but also the loci of quasars/AGNs in the near-infrared CCD. We finally discuss the possibility of contamination by other types of objects. We compare the locus of AGNs with an other four types of objects (namely, microquasars, cataclysmic variables, low mass X-ray binaries, and massive young stellar objects), which have a radiation mechanism similar to that of AGNs. In the near-infrared CCD, each type of object is located at a position similar to the stellar locus. Accordingly, it is highly probable that we can differentiate between the four types of objects on the basis of their locus in a near-infrared CCD. We additionally consider contamination by distant normal galaxies. The near-infrared colours of several types of galaxies are also simulated using the Hyperz code. Although galaxies with $z \sim 1$ have near-infrared colours similar to those of AGNs, these galaxies are unlikely to be detected because they are very faint. In other words, few galaxies should contaminate the locus of AGNs in the near-infrared CCD. Consequently, we can extract reliable AGN candidates on the basis of the near-infrared CCD.

Key words. galaxies: active – quasars: general – catalogs

1. Introduction

Active galactic nuclei (AGNs) are tremendous energetic sources, where vast amounts of energy are generated by gravitational accretion of mass around a supermassive black hole. The radiation at nearly all wavelengths enables us to detect AGNs in multiwavelength observations. Hence, AGNs have been studied at various wavelengths. Past studies show that their spectral energy distributions (SEDs) are roughly represented by a power-law (i.e., $f_\nu \propto \nu^{-\alpha}$), whilst normal galaxies have an SED that peaks at ∼1.6 μm and resembles the composite black-body spectra of the stellar population. Because the colours of an object provide us with rough but essential information about its spectrum, colours are important tools for differentiating AGNs from normal stars.

Colour selection is an efficient technique for distinguishing AGNs from normal stars and have played an important role in extracting AGN candidates without spectral observations. A classic method is known as the UV-excess (UVX; Sandage 1965; Schmidt & Green 1983; Boyle et al. 1990). The UVX technique exploits that quasars are relatively brighter than stars at shorter wavelengths and therefore occupy a bluer locus in a CCD with respect to stars. In addition, many AGN candidates have been selected on the basis of colours at various wavelengths: optical (Richards et al. 2002), optical and near-infrared (Glikman et al. 2007), and mid-infrared (Lacy et al. 2004; Stern et al. 2005). These studies provide us with clues about the properties of AGNs.

Target selection of high redshift quasars has also been performed using their colours, mainly at optical wavelengths (e.g., Fan et al. 2000, 2001, 2003). However, near-infrared properties are required when attempting to select targets such as higher redshift quasars, since the shift of the Lyman break to longer wavelengths makes observations difficult at optical wavelengths. Therefore, near-infrared selection should be a useful technique for extracting high-redshift quasars.

In this paper, we present a study of the near-infrared colours of AGNs and demonstrate, by using both observed and simulated colours, that near-infrared colours can help us to differentiate between AGNs and normal stars. In addition, we predict near-infrared colour evolution based on a Monte Carlo simulation. In Sect. 2, we introduce the catalogues of AGNs, which are used to investigate the observed colours. We confirm the near-infrared properties of spectroscopically confirmed AGNs on the basis of the near-infrared CCD and redshift-colour relations in Sect. 3. In Sect. 4, we simulate the near-infrared colours using the Hyperz code developed by Bolzonella et al. (2000) and demonstrate that AGNs reside in a distinct position in the near-infrared CCD. In Sect. 5, we consider other probable objects that are expected to have near-infrared colours similar to those of AGNs.

2. Data

We examine the near-infrared properties of quasars/AGNs using 2MASS magnitudes. The samples of quasars/AGNs are extracted from the Sloan Digital Sky Survey Data Release 5 (SDSS-DR5) quasar catalog and the catalogue of Quasars and Active Galactic Nuclei (12th edn.), which are both briefly introduced below.

2.1. 2MASS

The Two Micron All Sky Survey (2MASS[1]; Skrutskie et al. 2006) is a project that observed 99.998% of the entire sky at the J (1.25 μm), H (1.65 μm), and Ks (2.16 μm) bands, at Mt. Hopkins, Arizona, USA (in the northern hemisphere) and at CTIO, Chile (in the southern hemisphere) between June 1997 and February 2001. The instruments are both highly automated 1.3-m telescopes equipped with three-channel cameras, each channel consisting of a 256 × 256 array of HgCdTe detectors. The 2MASS obtained 4 121 439 FITS images (pixel size ~2.″0) with 7.8 s of integration time. The 10σ point-source detection levels are fainter than 15.8, 15.1, and 14.3 mag at J, H, and K_S bands. The Point Source Catalogue (PSC) was produced using these images and catalogued 470 992 970 sources. At the 2MASS website, the images and the PSC are easily available to the public.

2.2. SDSS-DR5 quasar catalog

The Sloan Digital Sky Survey (SDSS) provides a photometrically and astrometrically calibrated digital imaging survey of π sr above Galactic latitude 30° in five broad optical bands to a depth of $g' \sim 23$ mag (York et al. 2000). Many astronomical catalogues have been produced by this survey.

The SDSS quasar catalog IV (Schneider et al. 2007, hereafter SQ) is the fourth edition of the SDSS quasar catalog I (Schneider et al. 2002), which is selected from the SDSS-DR5 (Adelman-McCarthy et al. 2007). The SQ catalogue consists of 77 429 quasars, the vast majority of which were discovered by the SDSS. The area covered by the catalogue is ≈5740 deg^2. The quasar redshifts range from 0.08 to 5.41, with a median value of 1.48. The positional accuracy of each object is superior to 0.″2.

2.3. Quasars and active galactic nuclei (12th edn.)

The catalogue of quasars and active galactic nuclei (12th edn.) (Véron-Cetty & Véron 2006, hereafter QA) is the 12th edition of the catalogue of quasars first published in 1971 by De Veny et al. The QA catalogue consists of 85 221 quasars, 1122 BL Lac objects, and 21 737 active galaxies (including 9628 Seyfert 1), and includes position and redshift data as well as optical brightness (U, B, V) and 6 cm and 20 cm flux densities when available. The positional accuracy is superior to 1.″0.

3. Near-infrared properties of AGNs

3.1. Extraction of near-infrared counterparts

The sources in two of the above-mentioned AGN catalogues (SQ and QA) were cross-identified with the 2MASS PSC, and we extracted the near-infrared counterpart of each source. As mentioned in the previous section, the positional accuracies of both catalogues are superior to 1″. Therefore, we identified an near-infrared counterpart when a 2MASS source was located within 1″ of a SQ/QA position.

As a result of the extraction, we derived 9658 (SQ catalogue) and 14 078 (QA catalogue) near-infrared counterparts. For investigating the near-infrared properties using 2MASS magnitudes, we used only 2817 (SQ) and 7061 (QA) objects, where 2MASS photometric quality flags are superior to B (signal-to-noise ratio $(S/N) > 7\sigma$).

[1] 2MASS website (http://www.ipac.caltech.edu/2mass/).

3.2. Colour–colour diagram

The near-infrared $(H - K_S) - (J - H)$ CCD is a powerful tool for investigating the properties of celestial objects. We investigated the near-infrared properties of quasars/AGNs using a near-infrared CCD.

Figure 1 shows the distributions of quasars/AGNs in a $(H - K_S) - (J - H)$ CCD. In previous studies, the intrinsic loci of stars and classical T Tauri stars (CTTS) were clearly defined by Bessell & Brett (1988) and Meyer et al. (1997). Their loci are also shown in the CCD. Bessell & Brett (1988) and the Caltech (CIT) systems are transformed into the 2MASS photometric system by the method introduced by Carpenter (2001). The reddening vector, taken from Rieke & Lebofsky (1985), is also shown in the diagram. Because the stellar and CTTS loci can only shift along the reddening vector, most of these types of stars fundamentally should not be located in the region described by the following equations:

$$(J - H) \leq 1.70(H - K_S) - 0.118. \quad (1)$$

$$(J - H) \leq 0.61(H - K_S) + 0.50. \quad (2)$$

Equation (1) represents the lower-limit line to where normal stars can reside and Eq. (2) represents the lower-limit line to where CTTS can reside. Both lines are also shown in Fig. 1. Below, we call the region enclosed by Eqs. (1) and (2) "region II" and all other regions "region I". In Fig. 1, we can see that most of the quasar/AGNs are located in clearly different areas than the stellar loci. The distributions of the quasar/AGNs are on the right side of the stellar loci in the CCD, i.e., they have a $(J-H)$ colour similar to that of normal stars but have a $(H - K_S)$ colour redder than that of normal stars. Table 1 counts the number of objects in each region. It shows that 70% of AGNs and 80% of quasars are distributed in region II. Hence, the near-infrared selection of quasars can be more effective than that of other types of AGN. In particular, ~90% of low redshift quasars with $0 \leq z \leq 1$ reside in region II, so these quasars are rarely missed. However, objects with $1 < z \leq 2$ or $4 < z \leq 5$ tend to have a bluer $(H - K_S)$ colour than objects with other redshift ranges, which is similar to the colour of normal stars. Therefore, some of these quasars/AGNs might be missed. The difference of the loci between quasars/AGNs and normal stars is probably caused by the difference in the radiation mechanism because the dominant type of radiation of quasars/AGNs is not black-body radiation.

This colour property was proposed to be caused by a K-excess by Warren et al. (2000), who developed a KX method where quasars with a $(V - J)$ colour similar to that of stars would be redder in $(J - K)$ colour. In other words, this KX method can separate quasars and stars on the basis of their colours. This technique was used for selecting quasar candidates (e.g., Smail et al. 2008; Jurek et al. 2008; Nakos et al. 2009). The present work is a variant of the original KX technique, using the $(J - H)$ versus $(H - K_S)$ diagram.

3.3. Colours versus redshift

In Fig. 2, we plot the SDSS quasars, in terms of three colours versus redshift, and their average colour evolution with redshift. The redshifts are taken from the SQ catalogue.

Each colour experiences only a small change or dispersion with redshift. This is probably due to the variety of spectral shapes and/or extinctions. In the near-infrared CCD, this small colour change causes a small variation in the AGN locus. These properties can be reproduced by the simulation as mentioned below.

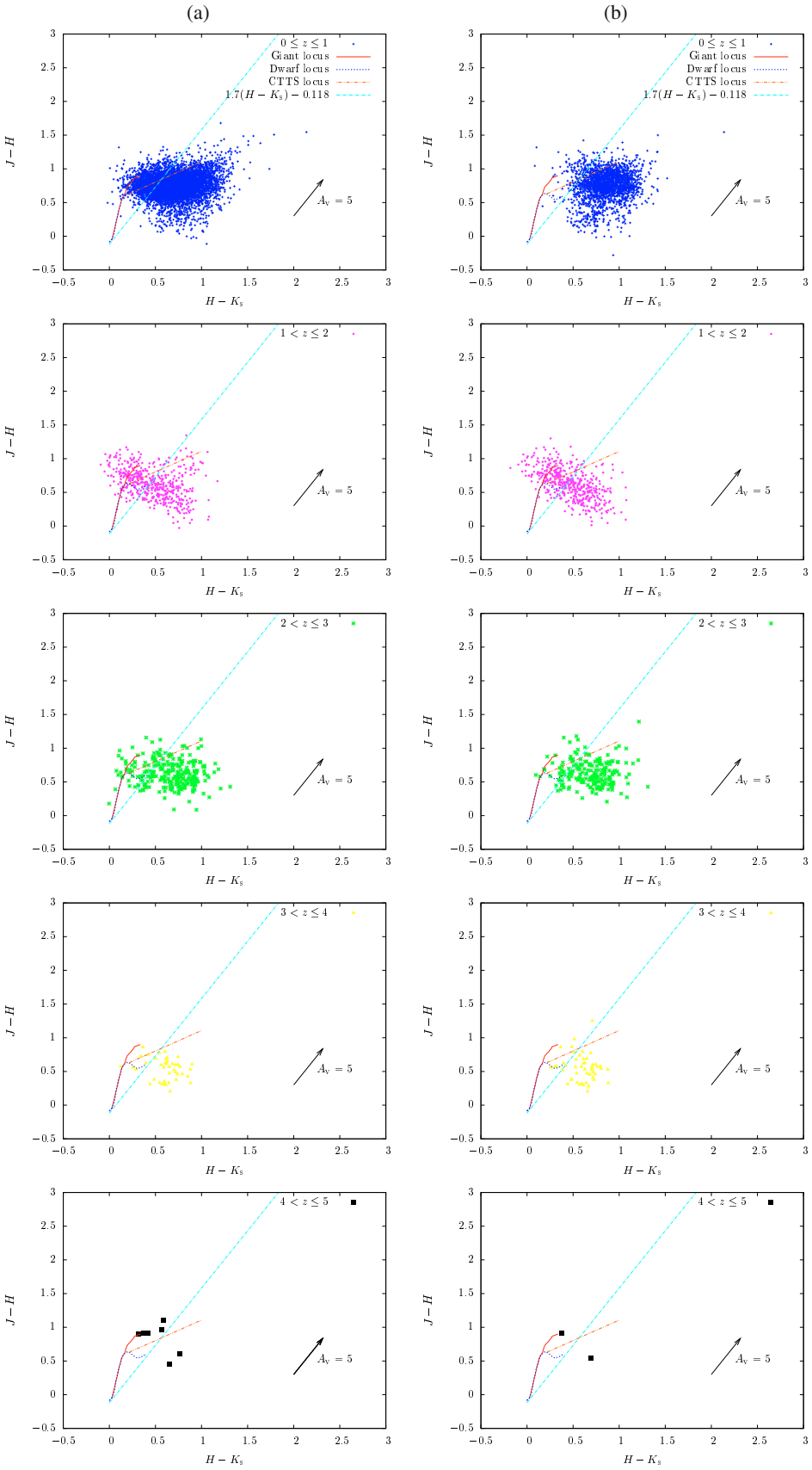

Fig. 1. a) The distribution of AGNs in the QA catalogue. **b)** The distribution of quasars in the SQ catalogue. The stellar locus (Bessell & Brett 1988), the CTTS locus (Meyer et al. 1997), and the reddening vector taken from Rieke & Lebofsky (1985) are also shown.

Table 1. The number of objects distributed in the regions I and II.

Redshift range	QA catalogue			SQ catalogue		
	region I	region II	total	region I	region II	total
$0 \le z \le 1$	1671 (27)	4480 (73)	6151	222 (11)	1869 (89)	2091
$1 < z \le 2$	238 (47)	265 (53)	503	222 (47)	249 (53)	471
$2 < z \le 3$	67 (25)	197 (75)	264	38 (19)	165 (81)	203
$3 < z \le 4$	7 (16)	36 (84)	43	9 (18)	41 (82)	50
$4 < z \le 5$	5 (71)	2 (29)	7	1 (50)	1 (50)	2
Total	1998 (29)	4970 (71)	6968	500 (18)	2317 (82)	2817

Of 7061 AGNs detected in the QA catalogue, 93 do not have a measured redshift. The values in parentheses represent percentages of quasars/AGNs residing in each region.

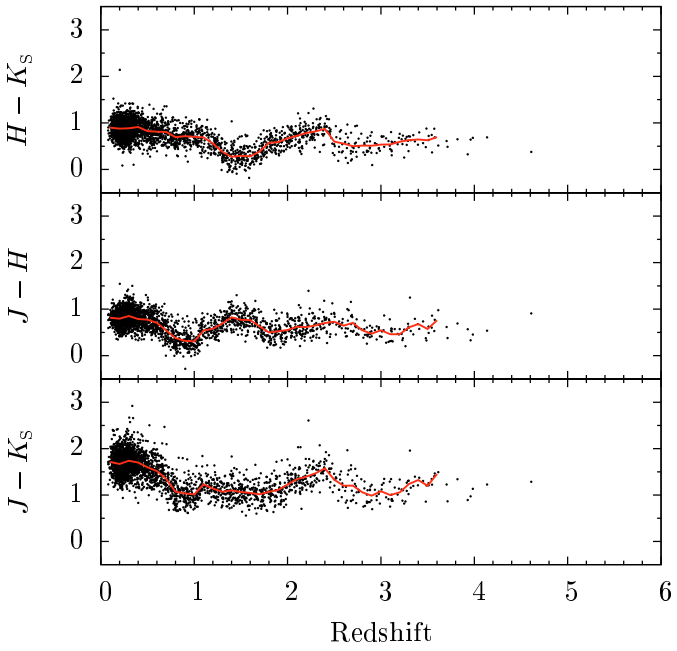

Fig. 2. Colours versus redshift for SDSS quasars. The redshifts are taken from the SQ catalogue. The red solid lines show the average colour evolution with respect to redshift.

4. Simulating the near-infrared colours of quasars

We demonstrate that the locus of quasars is well separated from that of normal stars on the basis of a simulation using a realistic SED of quasars.

To simulate the near-infrared colours of quasars, we performed a Monte Carlo simulation with Hyperz code (Bolzonella et al. 2000). The Hyperz code calculates photometric redshifts using spectral template library, which identifies the best-fit SED by minimizing the χ^2 derived by comparing the observed SED with the expected SEDs. The reddening effects are taken into account according to a selected reddening law. Although this code is usually used for estimating photometric redshifts, we use it to derive the near-infrared colours at various redshifts.

We first made a magnitude list containing randomly generated J, H, K_S magnitudes, ranging from 8 to 16 mag (roughly coincident with a reliable range of 2MASS magnitude) and produced 100 000 data sets. These data sets were fitted by various model SED using the Hyperz code. A realistic SED of quasars was taken from Polletta et al. (2007) (i.e., QSO1 in Polletta et al. 2007). According to Polletta et al. (2007), the SED of the QSO1 is derived by combining the SDSS quasar composite spectrum and rest-frame IR data of a sample of 3 SDSS/SWIRE quasars (Hatziminaoglou et al. 2005). We used the reddening law from Calzetti et al. (2000), which is included by default in the Hyperz code. After inputting the data sets into the Hyperz code, we derived photometric redshifts with the probabilities associated with the value of χ^2. We only used objects with probabilities of ≥99%.

Figure 3 shows the simulated colour evolution with redshift. The curves in each diagram represent the simulated colours with $A_V = 0$–4 (from bottom to top), respectively. To find the best-fits to the average colour curves, we performed Kolmogorov-Smirnov (KS) tests between the average colour curves and each simulated colour curve. Table 2 shows the result of the KS tests. In all three colours, the colour evolution with $A_V = 2$ is the best-fit to each of the five A_V values. In addition, the redshift-colour relations of SQ quasars can be roughly reproduced by simulated curves with $0 \lesssim A_V \lesssim 3$. A variety of extinctions probably generate the dispersion in the colours. It should be noted that both the $(J - H)$ and $(J - K_S)$ colours steeply increase above redshift $z \sim 9$. This is due to shifting of the Lyman break into the J-band wavelength range. This property can be useful for extracting high-redshift quasars.

In Fig. 4, the simulated colours with $A_V = 2$ are shown in the $(H - K_S) - (J - H)$ CCD, tracked by redshift evolution. An important point is that the simulated position is separated well from the stellar locus, that is, it is consistent with the loci of quasars/AGNs shown in Fig. 1. A variety of types of extinction causes a dispersion in the simulated position and this can probably reproduce the dispersion in the loci of quasars/AGNs in Fig. 1. It is also consistent with the quasars with $0 \le z \le 1$ having relatively redder colours in $(H-K_S)$ than the quasars with $1 \le z \le 2$.

Although it is difficult to identify high-redshift quasars at $z \lesssim 8$, we can extract high-redshift quasar candidates at $z \gtrsim 8$ on the basis of a $(H-K_S)-(J-H)$ diagram because the $(J-H)$ colour steeply increases above $z \sim 8$.

5. Discussion

5.1. Other probable objects

Although the locus of AGNs in the near-infrared CCD differs from that of normal stars, other types of objects might be distributed in the locus with properties similar to those of AGNs. If a position in the CCD depends on the radiation mechanism, other objects with radiation mechanisms similar to AGNs are also expected to be located at the same position. Below, we examine further the loci of four types of objects that emit non-thermal radiation or are considered to be bright at both near-infrared and X-ray wavelengths: microquasars, cataclysmic

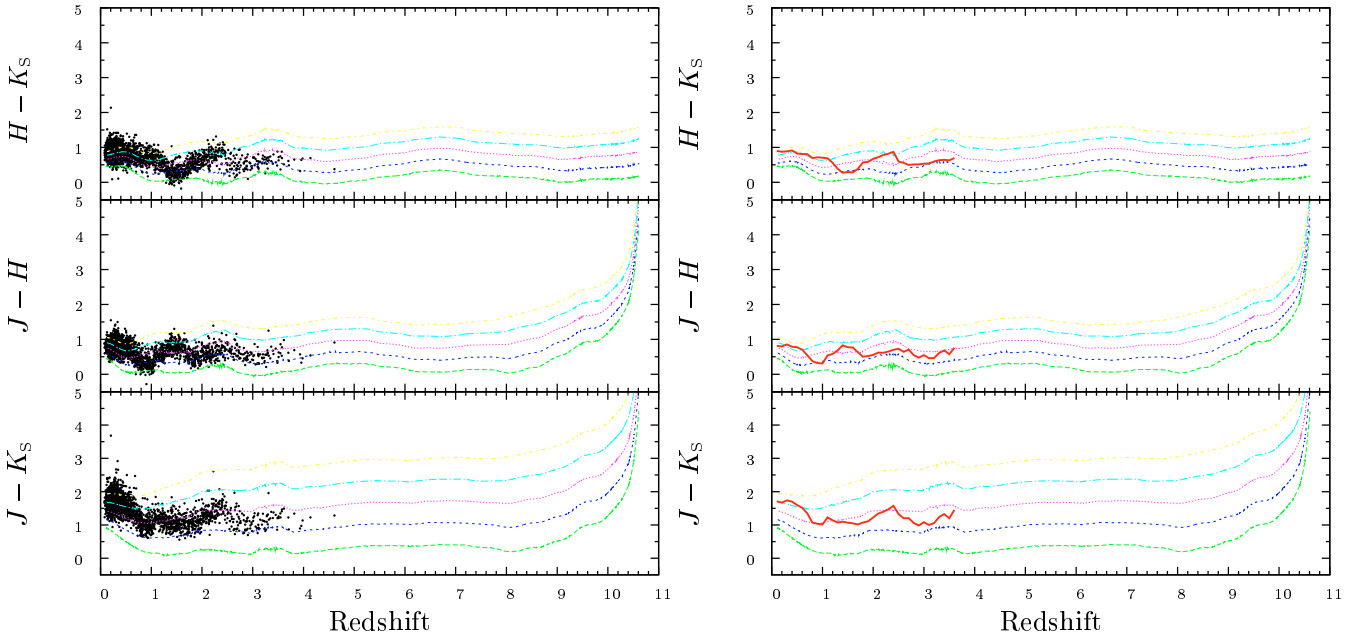

Fig. 3. Simulated colours versus redshift. The curves represent the simulated colour evolution with $A_V = 0, 1, 2, 3, 4$ (*from bottom to top*), respectively. The SDSS quasars (*left panel*) and the average colour evolution (*right panel*) shown in Fig. 2 are also plotted in the diagram.

Table 2. Results of a KS test between average colour evolution and simulated colour evolution.

A_V	$J - K_S$	$J - H$	$H - K_S$
0	0.78 (0)	0.94 (0)	0.86 (0)
1	0.94 (0)	0.69 (0)	0.60 (0)
2	0.26 (17)	0.29 (9)	0.14 (84)
3	0.79 (0)	0.82 (0)	0.59 (0)
4	1.0 (0)	1.0 (0)	0.88 (0)

The decimal values represent KS distance between two data and the values in parentheses represent significance level (percentage) for each KS test.

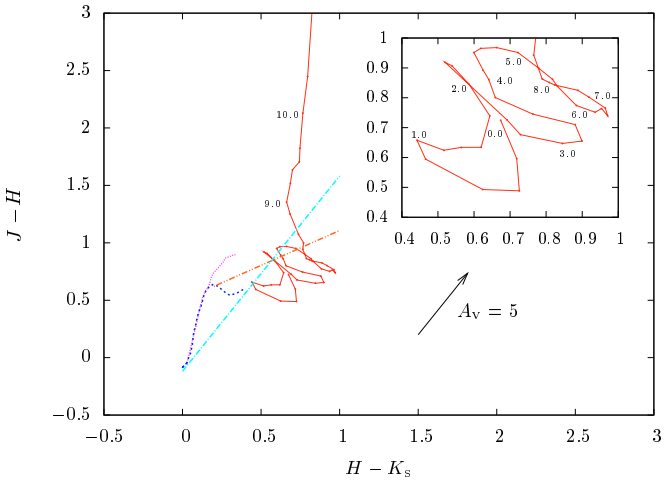

Fig. 4. Simulated colour evolution with redshift in the $(H - K_S) - (J - H)$ diagram. The stellar locus and the reddening vector are also shown in the diagram, which are the same as in Fig. 1.

variables (CVs), low mass X-ray binaries (LMXBs), and massive young stellar objects (MYSOs).

Sample objects are extracted from three catalogues, namely microquasar candidates (microquasars; Combi et al. 2008), cataclysmic binaries, LMXBs, and related objects (CVs and LMXBs; Ritter & Kolb 2003b), and catalogue of massive young stellar objects (MYSOs; Chan et al. 1996). First, we cross-identified each catalogue with 2MASS PSC, and extracted the near-infrared counterparts. Combi et al. (2008) cross-identified their catalogue with the 2MASS catalogue by adopting a cross-identification of 4″. The positional accuracy in the catalogue of Ritter & Kolb is ∼1″ (Ritter & Kolb 2003a). The objects in the MYSO catalogue were selected from the Infrared Astronomical Satellite (IRAS) PSC, whose typical position uncertainties are between about 2″ and 6″ (Beichman et al. 1988; Helou et al. 1988). Therefore, we set positional criteria for the cross-identification to be ≤2″ (CV and LMXB catalogues) and ≤4″ (microquasar and MYSO catalogues). We used objects with a 2MASS photometric quality superior to B (i.e., $S/N > 7\sigma$). Using their 2MASS magnitudes, they were plotted in a $(H - K_S) - (J - H)$ diagram.

Figure 5 shows the CCD of each object. In each case, a few objects were distributed around the locus of the AGNs, although most objects were distributed around the stellar locus or reddened region of the stellar locus. Table 3 lists the number and percentage of objects distributed in each region. Although the percentages of both CVs and LMXBs that reside in region II are relatively higher than those of the other two types of objects, they are not greater than ∼25%. In addition, few objects have $(H - K_S) \sim 0.8$ in the region II, although most quasars/AGNs have this colour (see Fig. 1). Accordingly, contamination by these four types of objects should be a small fraction.

This means that the dominant radiation of the four objects should be thermal radiation. The AGNs also radiate thermal radiation, but it represents a very small fraction compared to the non-thermal component produced by accretion around supermassive black holes. Therefore, AGNs should be well separated by these four objects using the near-infrared colours.

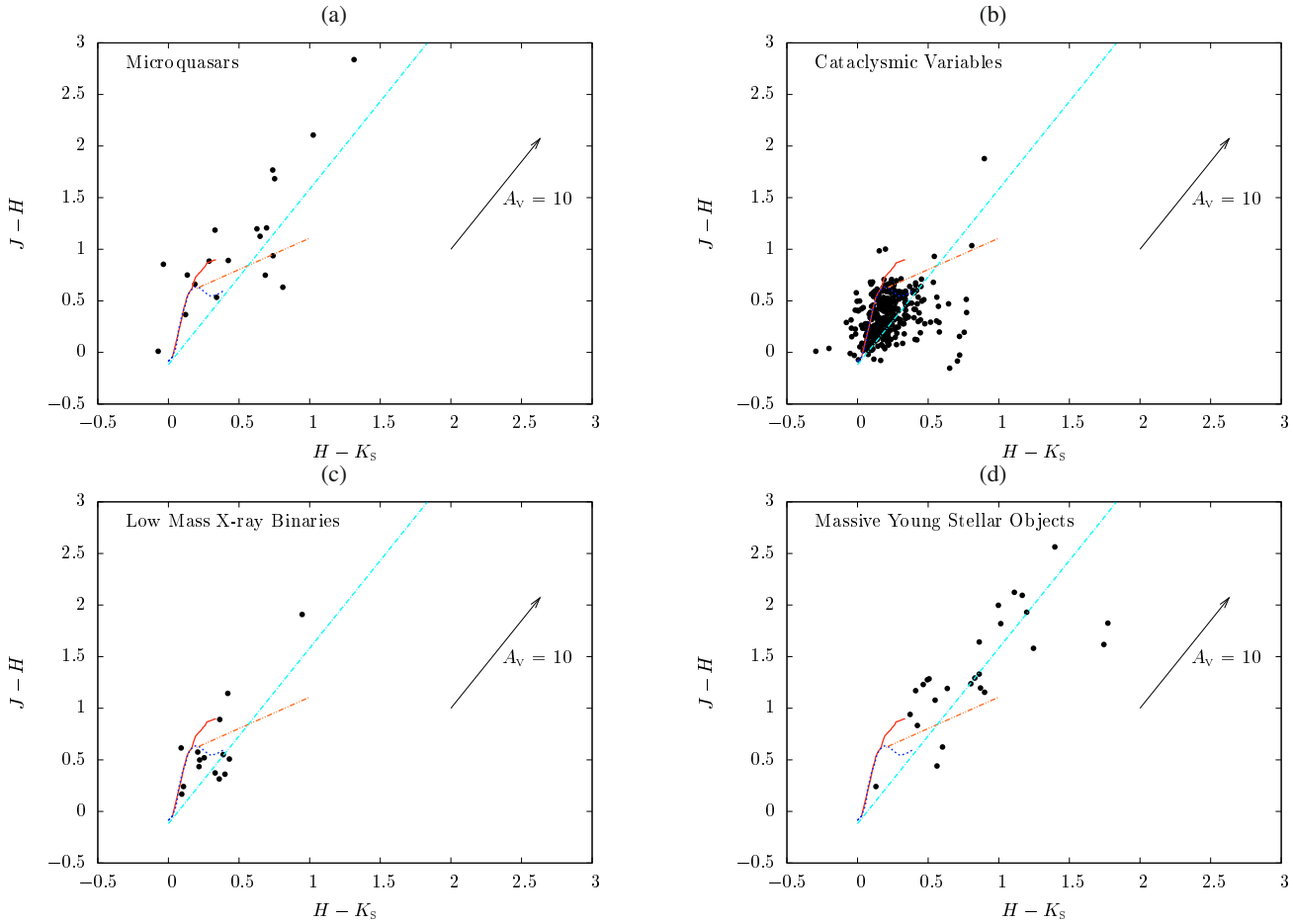

Fig. 5. The distribution of four types of objects: microquasars (*upper left*), cataclysmic variables (*upper right*), low mass X-ray binaries (*lower left*), and massive young stellar objects (*lower right*). The stellar locus and the reddening vector are the same as in Fig. 1.

Table 3. The number and percentage of objects distributed in each region.

	Microquasars	CV	LMXB	MYSO
I	16 (84)	245 (75)	11 (73)	27 (93)
II	3 (16)	82 (25)	4 (27)	2 (7)
Total	19	327	15	29

The values in parentheses represent percentage.

5.2. Contamination by normal galaxies

Distant galaxies that appear as point-like sources might contaminate the AGN locus in the near-infrared CCD. We confirmed the locus of normal galaxies in the near-infrared CCD by performing a Monte Carlo simulation as in Sect. 4. The SED templates we used are seven spiral galaxies in Polletta et al. (2007): spirals range from early to late types (S0-Sd).

Figure 6 shows the simulated intrinsic colours (i.e., $A_V = 0$) of the seven galaxies. Galaxies with $0 \leq z \lesssim 0.8$ have intrinsic colours similar to those of normal stars (i.e., they are in the region I). Galaxies with $1.4 \lesssim z \leq 3$ are distributed around the reddened region of either normal stars and/or CTTS. Therefore, they should not be mistaken for AGN candidates. On the other hand, simulated colours with $z \sim 1$ are located in the region II. A fraction of AGN in the region II are possibly mistaken for galaxies with $z \sim 1$. However, galaxies at $z \sim 1$ should not have enough brightness to be detected with mid-scale telescopes.

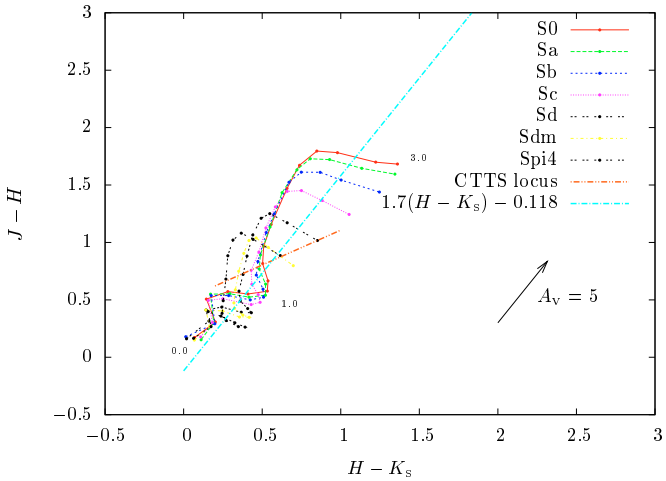

Fig. 6. Simulated colour evolution for seven spiral galaxies. Redshift ranges from 0.0 to 3.0 with $\Delta z = 0.2$ interval points. The boundary between regions I and II is also drawn in the diagram.

Even the brightest galaxy has no more than $M \sim -23$ mag at SDSS r-band (Blanton et al. 2001; Baldry et al. 2004). If such a galaxy were located at $z \sim 1$, its apparent magnitude would be $m \gtrsim 20$ mag at J-band. In addition, the apparent magnitude would be even fainter because most galaxies have $M > -23$ mag and the apparent brightness suffers extinction. Accordingly, only

large-scale telescopes can observe these galaxies. Hence, few galaxies should contaminate the AGN locus in the near-infrared CCD with respect to the data where limiting magnitude is below 20 mag.

6. Summary and conclusion

We have confirmed the existence of a loci of catalogued quasars/AGNs in a $(H - K_S) - (J - H)$ diagram, of which above 70−80% are clearly separated from the stellar locus. In addition, we have simulated the near-infrared colours of quasars on the basis of a Monte Carlo simulation with Hyperz code, and demonstrated that the simulated colours can reproduce both the redshift-colour relations and the locus of quasars in the near-infrared CCD. We have also predicted the colour evolution with redshift (up to $z \sim 11$). Finally, we have discussed the possibility of contamination by other types of objects. The locus of AGNs also differs from those of the other four probable types of objects (namely, microquasars, CVs, LMXBs, MYSOs) that are expected to be located within similar loci. We also demonstrated with a Monte Carlo simulation that normal galaxies are unlikely to contaminate the locus of AGNs in the near-infrared CCD.

Hewett et al. (2006) investigated near-infrared colours of quasars using an artificial SED, but we have proposed near-infrared colour selection criteria for extracting AGNs and studied both observed and simulated colours, presenting quantitative discussions. An important point is that our selection criteria require only near-infrared photometric data, although some previous studies (e.g., Glikman et al. 2007, 2008) adopted colour selections based on colours between near-infrared and optical wavelengths. In other words, our selection criteria make the extraction of candidates easier because only near-infrared colours are required. This technique should also be useful when searching for high-redshift quasars, since they become very faint at optical wavelength due to the shift in their Lyman break.

This paper demonstrates that near-infrared colours can be useful for selecting AGN candidates. If an additional constraint is imposed, more reliable candidates can be extracted. When using the near-infrared colour selection with an additional constraint on near-infrared catalogues containing sources distributed across a large area (e.g., 2MASS, DENIS, UKIDSS, and future surveys), many AGN samples (possibly over ∼10 000) are expected to be derived in a region over ∼10 000 deg^2. Kouzuma & Yamaoka (2009a) (see also Kouzuma & Yamaoka 2009b) cross-identified the 2MASS PSC with the ROSAT catalogue, and extracted AGN candidates across the entire sky using the near-infrared colour selection in this paper. These large number of samples may provide us with clues about such an evolution of AGNs and X-ray background. Additionally, in our simulation, quasars with $z \gtrsim 8$ can be extracted on the basis of near-infrared colours. This property might be helpful for searching for high-redshift quasars in the future.

Acknowledgements. This publication makes use of data products from the Two Micron All Sky Survey, which is a joint project of the University of Massachusetts and the Infrared Processing and Analysis Center/California Institute of Technology, funded by the National Aeronautics and Space Administration and the National Science Foundation. Funding for the SDSS and SDSS-II has been provided by the Alfred P. Sloan Foundation, the Participating Institutions, the National Science Foundation, the US Department of Energy, the National Aeronautics and Space Administration, the Japanese Monbukagakusho, the Max Planck Society, and the Higher Education Funding Council for England. The SDSS Web Site is http://www.sdss.org/. We thank the anonymous referee for useful comments to improve this paper.

References

Adelman-McCarthy, J. K., Agüeros, M. A., Allam, S. S., et al. 2007, ApJS, 172, 634
Baldry, I. K., Glazebrook, K., Brinkmann, J., et al. 2004, ApJ, 600, 681
Beichman, C. A., Neugebauer, G., Habing, H. J., et al. 1988, Infrared astronomical satellite (IRAS) catalogs and atlases, Explanatory supplement, 1
Bessell, M. S., & Brett, J. M. 1988, PASP, 100, 1134
Blanton, M. R., Dalcanton, J., Eisenstein, D., et al. 2001, AJ, 121, 2358
Bolzonella, M., Miralles, J.-M., & Pelló, R. 2000, A&A, 363, 476
Boyle, B. J., Fong, R., Shanks, T., & Peterson, B. A. 1990, MNRAS, 243, 1
Calzetti, D., Armus, L., Bohlin, R. C., et al. 2000, ApJ, 533, 682
Carpenter, J. M. 2001, AJ, 121, 2851
Chan, S. J., Henning, T., & Schreyer, K. 1996, A&AS, 115, 285
Combi, J. A., Albacete-Colombo, J. F., & Martí, J. 2008, A&A, 477, 125
Fan, X., White, R. L., Davis, M., et al. 2000, AJ, 120, 1167
Fan, X., Narayanan, V. K., Lupton, R. H., et al. 2001, AJ, 122, 2833
Fan, X., Strauss, M. A., Schneider, D. P., et al. 2003, AJ, 125, 1649
Glikman, E., Helfand, D. J., White, R. L., et al. 2007, ApJ, 667, 673
Glikman, E., Eigenbrod, A., Djorgovski, S. G., et al. 2008, AJ, 136, 954
Hatziminaoglou, E., Pérez-Fournon, I., Polletta, M., et al. 2005, AJ, 129, 1198
Helou, G., Walker, D. W., Helou, G., & Walker, D. W. 1988, Infrared astronomical satellite (IRAS) catalogs and atlases, The small scale structure catalog, 7
Hewett, P. C., Warren, S. J., Leggett, S. K., & Hodgkin, S. T. 2006, MNRAS, 367, 454
Jurek, R. J., Drinkwater, M. J., Francis, P. J., & Pimbblet, K. A. 2008, MNRAS, 383, 673
Kouzuma, S., & Yamaoka, H. 2009a, MNRAS, submitted
Kouzuma, S., & Yamaoka, H. 2009b, in ASP Conf. Ser. 411, ed. D. A. Bohlender, D. Durand, & P. Dowler, 426
Lacy, M., Storrie-Lombardi, L. J., Sajina, A., et al. 2004, ApJS, 154, 166
Meyer, M. R., Calvet, N., & Hillenbrand, L. A. 1997, AJ, 114, 288
Nakos, T., Willis, J. P., Andreon, S., et al. 2009, A&A, 494, 579
Polletta, M., Tajer, M., Maraschi, L., et al. 2007, ApJ, 663, 81
Richards, G. T., Fan, X., Newberg, H. J., et al. 2002, AJ, 123, 2945
Rieke, G. H., & Lebofsky, M. J. 1985, ApJ, 288, 618
Ritter, H., & Kolb, U. 2003a, VizieR Online Data Catalog, 5113, 0
Ritter, H., & Kolb, U. 2003b, A&A, 404, 301
Sandage, A. 1965, ApJ, 141, 1560
Schmidt, M., & Green, R. F. 1983, ApJ, 269, 352
Schneider, D. P., Richards, G. T., Fan, X., et al. 2002, AJ, 123, 567
Schneider, D. P., Hall, P. B., Richards, G. T., et al. 2007, AJ, 134, 102
Skrutskie, M. F., Cutri, R. M., Stiening, R., et al. 2006, AJ, 131, 1163
Smail, I., Sharp, R., Swinbank, A. M., et al. 2008, MNRAS, 389, 407
Stern, D., Eisenhardt, P., Gorjian, V., et al. 2005, ApJ, 631, 163
Véron-Cetty, M.-P., & Véron, P. 2006, A&A, 455, 773
Warren, S. J., Hewett, P. C., & Foltz, C. B. 2000, MNRAS, 312, 827
York, D. G., Adelman, J., Anderson, Jr., J. E., et al. 2000, AJ, 120, 1579